J. Plasma Physics (2002), *vol.* 68, *part* 1, *pp.* 59–73.
DOI: 10.1017/S0022377802001782 Printed in the United Kingdom

MHD analysis of the current-driven flute instability of a plasma

I. F. SHAIKHISLAMOV

Department of Laser Plasmas, Institute of Laser Physics, Novosibirsk 630090, Russia

(Received 1 March 2002)

Abstract. The lower-hybrid drift instability of a plasma driven by relative ion–electron motion is analyzed in the framework of the modified magnetohydrodynamic equations. The Hall contribution is expressed in terms that offer a simple physical interpretation of the process and allow a comprehensive study of various features and limits of instability. It is shown that in the chosen terms there are clear-cut ranges of magnetosonic drift, lower-hybrid drift, and kinetic versions of instability that have different properties. It is shown for the first time that the instability may have, besides a flute-like structure, a cell-like one as well. On the basis of the performed analysis, a new classification of the phenomenon is offered.

1. Introduction

Of the numerous plasma instabilities, the one that manifests itself in a pronounced flute-like structuring of the plasma surface along magnetic field lines has a long-standing history of research, starting with theta-pinch experiments in the early 1970s. Later, it was observed in the active magnetospheric missions (AMPTE) and laser-produced plasma experiments of the 1980s. One of the distinguishing features of this instability is that it operates on spatial and inverse time scales smaller than the ion gyroradius and cyclotron frequency on the one hand, and larger than the electron gyroradius and cyclotron frequency on the other. This scaling, as well as a broad range of physical conditions under which the instability was observed, led to a certain dualism in theoretical approaches – kinetic and magnetohydrodynamic (MHD). In the ensuing discussion, it was established that all of these phenomena have a common origin – the lower-hybrid drift instability (LHDI) driven by relative electron–ion drift. Winske (1988) proposed that all the cases can be understood either as density drift or effective gravity drift LHDI, and described by the same dispersion equation. In later work, usually (see e.g. Huba et al. 1990) the most general kinetic-based dispersion equations were used to analyze those features of the instability (wavelength structure, saturation, and trends of nonlinear evolution) that are still not clearly understood and show significant discrepancies between theory and experiment.

The purpose of this work is to analyze the properties of various versions of the instability in the framework of the simplest and thus more tractable MHD equations. Rather then generalize, we shall try to point out essential differences between these versions and to find out the ranges where one or other works. Primarily, the MHD instability will be investigated (as opposed to the ion-kinetic one); this is the

instability that is likely to have the greatest effects on the plasma. In contrast to earlier work, the problem will be studied in terms of coupling between the drift wave due to current and magnetosonic or lower-hybrid waves – instead of effective gravity, density and gravity drift terms. Instead of the previously proposed MHD ordering based on the ion Larmor radius, the ion plasma length will be used as the basic spatial scale. It will be shown that the main parameter that governs the Hall-modified MHD equations is the relation between this length and the magnetic field gradient scale, and also that the relation between the magnetic field gradient scale and the density gradient scale determines the structure of the instability and the effect of thermal pressure. Also, it will be shown that the instability may or may not have a long-wavelength limit – a feature that can be quite important from the point of view of long-time evolution. The possibility of the instability having a cell-like structure (as opposed to the usually considered flute-like structure) will be considered for the first time. It will be argued that high above the instability threshold, the cell-like structure may be dominant, and that in an expanding plasma, the counterstreaming ion flows at the front may account for the usually observed well-pronounced flutes.

The paper is organized as follows. In Sec. 2, the MHD equations including the Hall term are derived in appropriate limits and geometry. A physical interpretation of the instability is also presented. In Sec. 3, the effects of thermal pressure are investigated, as well as the ranges of ion-kinetic instability. In Secs. 4 and 5, the short-wavelength limit and the spatial structure of instability are discussed. A new classification of the phenomenon is then presented and discussed in Sec. 6, followed by conclusions in Sec. 7.

2. Modified MHD equations

We start with the two-fluid MHD equations for ions and massless electrons:

$$\frac{\partial n_e}{\partial t} + \boldsymbol{\nabla} \cdot (\mathbf{V}_e n_e) = 0, \tag{2.1a}$$

$$\frac{\partial n_i}{\partial t} + \boldsymbol{\nabla} \cdot (\mathbf{V}_i n_i) = 0, \tag{2.1b}$$

$$M \frac{d\mathbf{V}_i}{dt} = e\mathbf{E} + \frac{e}{c}\mathbf{V}_i \times \mathbf{B} - \frac{1}{n_i}\boldsymbol{\nabla} p_i, \tag{2.1c}$$

$$\mathbf{E} + \frac{1}{c}\mathbf{V}_e \times \mathbf{B} + \frac{1}{en_e}\boldsymbol{\nabla} p_e = 0. \tag{2.1d}$$

We make the further approximation of quasineutrality ($n_e = n_i = n$) and ignore electromagnetic effects. Then, after combining with the Maxwell equations, the modified MHD equations (Krall and Trivelpiece 1973) follows as

$$\frac{\partial \mathbf{B}}{\partial t} = \boldsymbol{\nabla} \times (\mathbf{V} \times \mathbf{B}) - \boldsymbol{\nabla} \times \left(\frac{\mathbf{J} \times \mathbf{B}}{nc} \right) + \boldsymbol{\nabla} \times \left(\frac{c}{ne} \boldsymbol{\nabla} p \right), \tag{2.2a}$$

$$nM \frac{d\mathbf{V}}{dt} = \frac{\mathbf{J} \times \mathbf{B}}{c} - \boldsymbol{\nabla}(p_e + p_i), \tag{2.2b}$$

$$\frac{\partial n}{\partial t} + \boldsymbol{\nabla} \cdot (\mathbf{V} n) = 0. \tag{2.2c}$$

https://doi.org/10.1017/S0022377802001782 Published online by Cambridge University Press

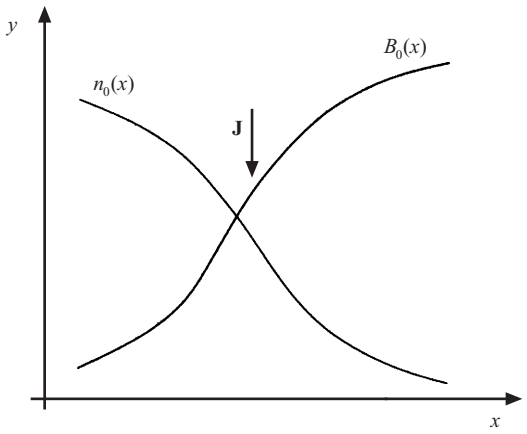

Figure 1. Geometry of the problem. The initial profiles of the density and magnetic field are shown.

We restrict the problem to two dimensions (x, y), with only one magnetic field component $\mathbf{B} = B\mathbf{h}_z$ (Fig. 1). The equations are simplified further to

$$\frac{\partial B}{\partial t} + \boldsymbol{\nabla} \cdot (\mathbf{V}B) = \frac{cB}{4\pi ne} \frac{\boldsymbol{\nabla} n \times \mathbf{h}_z}{n} \cdot \boldsymbol{\nabla} B, \tag{2.3a}$$

$$nM \frac{d\mathbf{V}}{dt} = -\frac{B}{4\pi} \boldsymbol{\nabla} B - \boldsymbol{\nabla} p, \tag{2.3b}$$

$$\frac{\partial n}{\partial t} + \boldsymbol{\nabla} \cdot (\mathbf{V}n) = 0. \tag{2.3c}$$

Here we have made use of the total plasma pressure $p = p_i + p_e$ and have neglected the term $\boldsymbol{\nabla} \times [(c/ne)\boldsymbol{\nabla} p_e]$, which is small if the electron beta is small and is exactly zero in the isothermal case. Equations (2.3) differ from the classic MHD ones only by the presence of the Hall term. The problem will be treated in slab geometry, assuming that initial gradients exist only along the x coordinate. Then we consider small perturbations $\propto \exp(-\mathbf{k}\cdot\mathbf{r})$ with wavevector $\mathbf{k}$ in a strong local approximation. This means that all terms of order $(kL)^{-1}$ and higher are ignored (here L is a characteristic gradient scale). For the normalized perturbations $\rho = \delta n/n_0$ and $b = \delta B/B_0$, it follows from (2.3) that

$$\frac{\partial b}{\partial t} - \frac{\partial \rho}{\partial t} = -V_j \left(\frac{\partial \rho}{\partial y} + \varepsilon \frac{\partial b}{\partial y} \right), \tag{2.4a}$$

$$\frac{\partial^2 \rho}{\partial t^2} = V_a^2 \nabla^2 b + C_s^2 \nabla^2 \rho, \tag{2.4b}$$

where V_a is the Alfvén velocity, $C_s = (\gamma p/n)^{1/2}$ is the thermal sound speed, $\varepsilon = -L_b/L_n$, and L_n and L_b are the gradient scales of the density and magnetic field. The relative speed between ions and electrons is given by

$$V_j = \frac{c}{4\pi n_0 e} \frac{dB_0}{dx}.$$

Usually, this is called the drift speed. However, one should remember that the drift velocity usually refers to the motion of the center of the particles' Larmor orbit, while here we have the total fluid velocity. The term $\partial\rho/\partial t$ in (2.4a) appeared from

https://doi.org/10.1017/S0022377802001782 Published online by Cambridge University Press

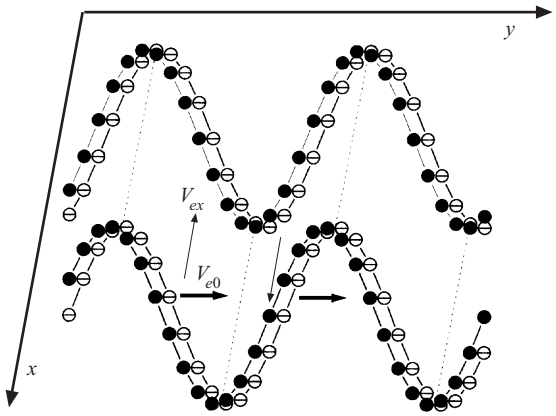

Figure 2. Electron motion in a perturbation.

substitution of $\nabla \cdot \mathbf{V}$ by $-n_0^{-1}\partial n/\partial t$. Note that a specification of the wave vector components k_x and k_y has not been made yet, since this is not necessary so far. It should be mentioned that the equations are written in the ion frame $V_{i0} = 0$. The final set of equations is strikingly simple. Without the term proportional to the drift speed, it describes a magnetosonic wave. In the chosen terms, the density drift speed is

$$\mathbf{V}_n \equiv \frac{\mathbf{h}_z \times \nabla p_i}{n\omega_{ci}} = \mathbf{V}_j \frac{2}{\gamma} c_s^2 \varepsilon.$$

Here $-c_s^2 = (C_s/V_a)^2 = \frac{1}{2}\gamma\beta$ is the square of the normalized sound speed, and we have assumed for simplicity that $L_{Ti} = L_n$ and $p_i = p$. The gravity drift speed can be expressed as

$$\mathbf{V}_g \equiv \frac{1}{\omega_{ci}} \mathbf{h}_z \times \frac{d\mathbf{V}_i}{dt} = \mathbf{V}_j - \mathbf{V}_n = \mathbf{V}_j \left(1 - \frac{2}{\gamma} c_s^2 \varepsilon\right).$$

Note that the vector $\mathbf{V}_j$ points in the $-y$ direction.

Before performing dispersion analyses, let us draw a physical picture of the process. Imagine that there appear ripples of density along the y axis (Fig. 2). Electrons have velocity V_{e0} relative to ions along the y axis and try to separate from them. If the magnetosonic speed is sufficiently small then the ions cannot catch up. In this case, the electric field E_y that builds up from charge separation induces electrons to move along the x axis in such a way as to compensate for the rapidly changing electron density. Then the ions start to move under the pressure of the ripples in the magnetic field that are generated by the component V_{ex} of the electron velocity. The time scale of their response is determined by the magnetosonic speed. If the magnetic field ripples compress ions further then a feedback of instability is established. Quantitatively, this line of reasoning is supported as follows. Compensating for the rapid change of electron density means that in the electron continuity equation the term

$$\nabla \cdot (n_e \mathbf{V}_e) = n_0 V_{e0} \frac{\partial \rho_e}{\partial y} + V_{ex} \frac{\partial n_0}{\partial x} + n_0 \nabla \cdot \mathbf{V}_e$$

should be zero. One can see that the main term $n_0 V_{e0}\, \partial \rho_e/\partial y$ can be balanced either by $n_0 \nabla \cdot \mathbf{V}_e$ or by $V_{ex}\partial n_0/\partial x$ if the density gradient is large enough. Both terms

https://doi.org/10.1017/S0022377802001782 Published online by Cambridge University Press

can be expressed through the magnetic field perturbation – the first from Ampère's law

$$V_{ex} = -\frac{cB_0}{4\pi n_0 e}\frac{\partial b}{\partial y}$$

and the second from the equation of magnetic field evolution:

$$\frac{\partial b}{\partial t} + (\mathbf{V}_e \cdot \boldsymbol{\nabla})b + \boldsymbol{\nabla} \cdot \mathbf{V}_e = \frac{\partial b}{\partial t} + (\mathbf{V}_i \cdot \boldsymbol{\nabla})b + \boldsymbol{\nabla} \cdot \mathbf{V}_e = 0, \quad \boldsymbol{\nabla} \cdot \mathbf{V}_e \approx -\frac{\partial b}{\partial t}.$$

Let us consider the first possibility:

$$n_0 V_{e0}\frac{\partial \rho_e}{\partial y} + n_0 \boldsymbol{\nabla} \cdot \mathbf{V}_e \approx 0.$$

Using Ampère's law, once again

$$V_{e0} \approx \frac{c}{4\pi n_0 e}\frac{\partial B_0}{\partial x} = \frac{cB_0}{4\pi n_0 e L_b}$$

and the equation

$$\frac{\partial^2 \rho}{\partial t^2} = V_a^2 \nabla_b^2$$

with the thermal pressure ignored, we obtain

$$\omega = V_a k_y \left(\frac{V_{e0}}{V_a}\right)^{1/3} \frac{1 + i\sqrt{3}}{2}, \qquad \rho = -\left(\frac{V_a}{V_{e0}}\right)^{2/3} \frac{1 + i\sqrt{3}}{2} b. \tag{2.5}$$

In the other case,

$$n_0 V_{e0}\frac{\partial \rho_e}{\partial y} + V_{ex}\frac{\partial n_0}{\partial x} \approx 0,$$

it follows that

$$\omega = V_a k_y \left(\frac{L_n}{L_b}\right)^{1/2}, \qquad b = \frac{L_n}{L_b}\rho. \tag{2.6}$$

It is evident that the first case (2.5) is dominant when the magnetic field gradient prevails, and is characterized by the relatively large magnetic field disturbance ($b \gg \rho$) and phase velocity ($\omega_r \approx \gamma$). In contrast, the second case (2.6) is dominant when the density gradient prevails. This wave is unstable only if the density and magnetic field gradients are opposite to each other, and is characterized by a relatively large density disturbance ($\rho \gg b$) and vanishing phase velocity ($\omega_r \ll \gamma$). The first case was recognized in Huba et al. (1990) as a new version of LHDI, while the second was termed by Hassam and Huba (1987) a modified Rayleigh–Taylor instability. According to the classification of Winske (1988), both cases are effective gravity drift instability (density gradient drift is ignored). In both cases, instability is driven by sufficiently large relative ion–electron velocity. As the current is supported by electromagnetic induction, so the energy for instability is derived from the magnetic energy. It is also clear that the instability can be interpreted as a coupling between the drift wave $\omega = -kV_j$ and the magnetosonic wave $\omega = -kV_a$. Therefore, there should be a threshold of the form $V_j \geqslant V_a$ that is independent of magnetic field strength – a feature pointed out for the first time in Hassam and Huba (1988).

The physical reasoning given above is supported by more rigorous analysis of (2.4). Let us consider first the simplest case of a cold plasma and a wave vector

https://doi.org/10.1017/S0022377802001782 Published online by Cambridge University Press

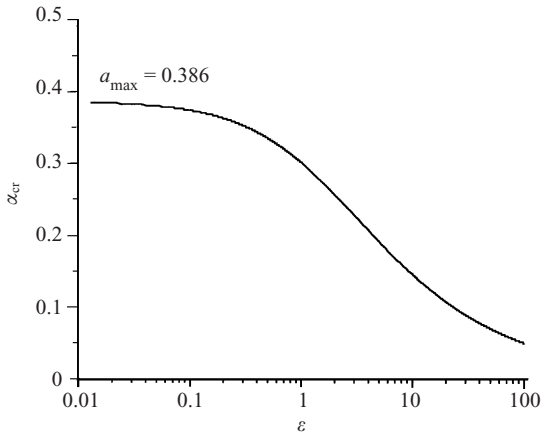

Figure 3. Critical value of $\alpha = V_j/V_a$ above which instability occurs, as a function of $\varepsilon = -L_b/L_n$.

having only a y component. The dispersion relation is then

$$x^3 - \alpha\varepsilon x^2 - x - \alpha = 0, \tag{2.7}$$

where

$$x = \frac{\omega}{k_y V_a}, \qquad \alpha = \frac{V_j}{V_a}.$$

The imaginary root appears when α is sufficiently large, and has two distinct limits. Either $\varepsilon \ll 1$, $x \approx (-\alpha)^{1/3}$ or $\varepsilon \gg 1$, $x \approx (-\varepsilon)^{-1/2}$. The critical value α_{cr} above which the system is unstable is shown in Fig. 3 as a function of ε. Actually, the threshold drift speed is only a relatively small fraction of the Alfvén velocity. Interestingly, the parameter α can be expressed not only in terms of velocities, but also in terms of spatial scales:

$$\alpha = \frac{V_j}{V_a} = \frac{\lambda_i}{L_b},$$

where $\lambda_i = c/\omega_{pi}$ is the ion plasma length.

3. Thermal pressure effects

In the framework of MHD, it is intuitively obvious that the thermal pressure should have a stabilizing effect. Indeed, it resists density clumping and, if large enough, it can balance the pressure of the magnetic field. The corresponding dispersion relation is

$$x^3 - \alpha\varepsilon x^2 - (1 + c_s^2)x - \alpha(1 - c_s^2\varepsilon) = 0. \tag{3.1}$$

It follows that in the case of a small density gradient ($\varepsilon = 0$), the only effect of the thermal pressure is to increase the instability threshold because of the increase in the magnetosonic speed. On the other hand, it has a quite dramatic effect on the Rayleigh–Taylor type of instability ($\varepsilon > 1$), because in this case, the density perturbation prevails and the thermal pressure may effectively resist the magnetic pressure. In Fig. 4, the critical value α_{cr} is shown as a function of ε at $c_s^2 = 0.5$. As one can see from (3.1), the wave becomes stable at $c_s^2 \approx \varepsilon^{-1}$. It should be

https://doi.org/10.1017/S0022377802001782 Published online by Cambridge University Press

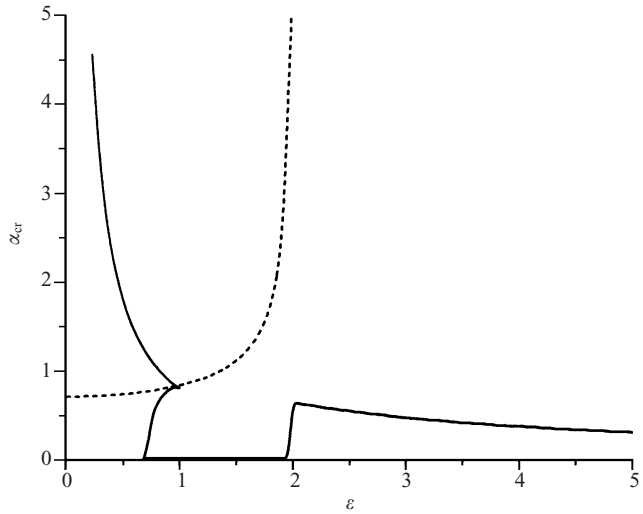

Figure 4. Thresholds of MHD (dashed curve) and kinetic (solid curve) instabilities as functions of ε for a given value of the thermal sound speed ($c_s^2 = 0.5$).

noted that this criterion nearly coincides (although not exactly) with the condition of large density drift – that is, when the plasma deceleration is small or is accelerated by thermal pressure overbalance ($V_g/V_n < 1$). However, in this case, the physics of instability quenching involves the thermal pressure, not the density drift.

The stabilizing effect of thermal pressure has been pointed out by many authors. Nevertheless, the general conclusion is that the plasma still remains unstable. The reason is that at finite temperature, inverse Landau damping becomes possible. Although to describe this effect, the ion response should be treated kinetically, its ranges still can be found in the framework of MHD. Inverse Landau damping occurs when there is a wave in the system that moves in the same direction as the ions but slower. The mean fluid velocity of ions in the laboratory frame is the diamagnetic velocity, which is the density drift: $V_{i0} = V_n$. Let $V_{\rm ph}$ be the phase velocity of the wave of (3.1). As this was obtained in the ion reference frame, it is $V_{\rm ph} + V_n$ in the laboratory frame. Inverse Landau damping is possible if $V_n < V_{\rm ph} + V_n < 0$. Note that in the chosen coordinate system, $V_n < 0$. It follows that a pair of conjugate roots of (3.1) are subject to instability – either MHD or kinetic (Fig. 5). In Fig. 4, the critical value $\alpha_{\rm cr}$ above which inverse Landau damping works is shown along with the range of MHD instability. As $\varepsilon c_s^2 \ll 1$ ($V_g/V_n \gg 1$, strong deceleration) MHD instability prevails, while at $\varepsilon c_s^2 \geqslant 1$ ($V_g/V_n < 1$, near equilibrium or plasma being accelerated), there is only kinetic instability. Besides this, when the density drift is smaller than but comparable to the gravity drift ($V_n/V_g < 1$; ($0.4 < \varepsilon c_s^2 < 1$, the left bound is approximate), kinetic instability is generated even at infinitely small $\alpha \to 0$. The same feature was also derived in kinetic analyses in the warm-ion limit (see e.g. Huba et al. 1990).

Kinetic instability derives energy from the thermal energy of ions, and in that respect it differs fundamentally from MHD instability. Also, the saturation mechanisms are physically different – nonlinear effects in the MHD case and modification of the ion distribution function in the kinetic case.

https://doi.org/10.1017/S0022377802001782 Published online by Cambridge University Press

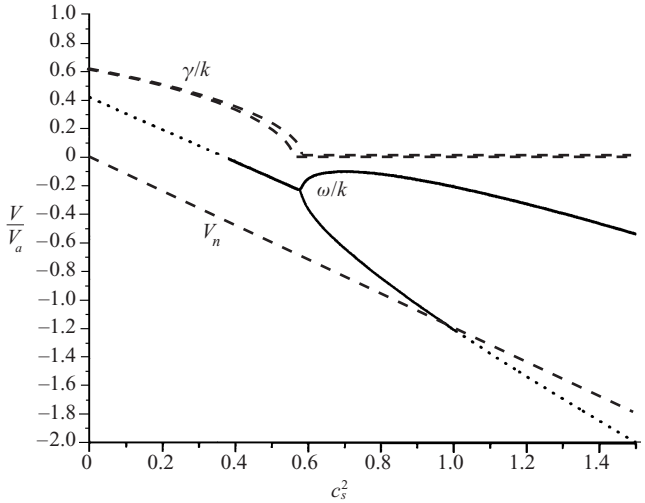

Figure 5. Diagram illustrating inverse Landau damping for $a = 1$ and $\varepsilon = 1$. The solid/dotted curve shows the phase velocity of the wave in the laboratory frame. The wave is kinetically unstable in the range $V_n < \frac{\omega}{k} < 0$ (solid) and stable otherwise (dotted). The dashed curves show the density drift V_n and the MHD growth rate of the wave.

4. Short-wavelength limit

As is well known, the magnetosonic wave transforms at $k > \lambda_e^{-1} \equiv \omega_{pe}/c$ into lower-hybrid oscillations: $\omega = \omega_H + kC_s$. Thus, one may expect that in MHD, the maximum grows rate is also restricted by $k_m \approx \omega_{pe}/c$ because of the weakening of the coupling between drift and magnetosonic waves. On the other hand, if the drift wave is relatively slow ($V_j < V_a$) and stable in the long-wavelength limit, then at large k ($V_j \geqslant V_a/k\lambda_e$), effective coupling with the lower-hybrid wave is possible. A physically simple way to include lower-hybrid effects is the following. At large k_y, the electron velocity V_{ex} becomes so large that the electron energy equals the ion energy. Therefore, one should reinstate the term $m\,dV_{ex}/dt \neq 0$ in the electron momentum equation. It is easy to see that this modifies the magnetic field equation (2.4a) in such a way that the time derivative $\partial b/\partial t$ should be replaced by

$$\frac{\partial b}{\partial t} - \left(\frac{\partial}{\partial t} - V_j \frac{\partial}{\partial y}\right) \lambda_e^2 \nabla^2 b.$$

Then the dispersion equation in the cold-plasma limit becomes

$$x^3(1 + k^2\lambda_e^2) - \alpha x^2(\varepsilon - k^2\lambda_e^2) - x - \alpha = 0. \tag{4.1}$$

This is exactly the same as derived for example in Winske (1988), in the limit of quasineutrality, and differs only in the definition of the terms. The dependence of the growth rate and real frequency of the wave on wavelength for various $\alpha \geqslant 1$ and ε is shown in Fig. 6. As one can see, at the maximum growth rate (which is of the order of the lower-hybrid frequency), the real frequency is always large. At sufficiently large k_y, unstable magnetosonic wave transforms to the stable lower-hybrid oscillations. The wavenumber at the maximum growth rate scales as $k_m\lambda_e \approx 1$ for $\varepsilon < 1$ and $k_m\lambda_e \approx \varepsilon^{1/2}$ for $\varepsilon > 1$.

Now, at sufficiently large $k\lambda_e \gg 1$, there appears an unstable wave even at very small α. For $\varepsilon = 0$, the maximum growth rate and corresponding wavenumber scale

https://doi.org/10.1017/S0022377802001782 Published online by Cambridge University Press

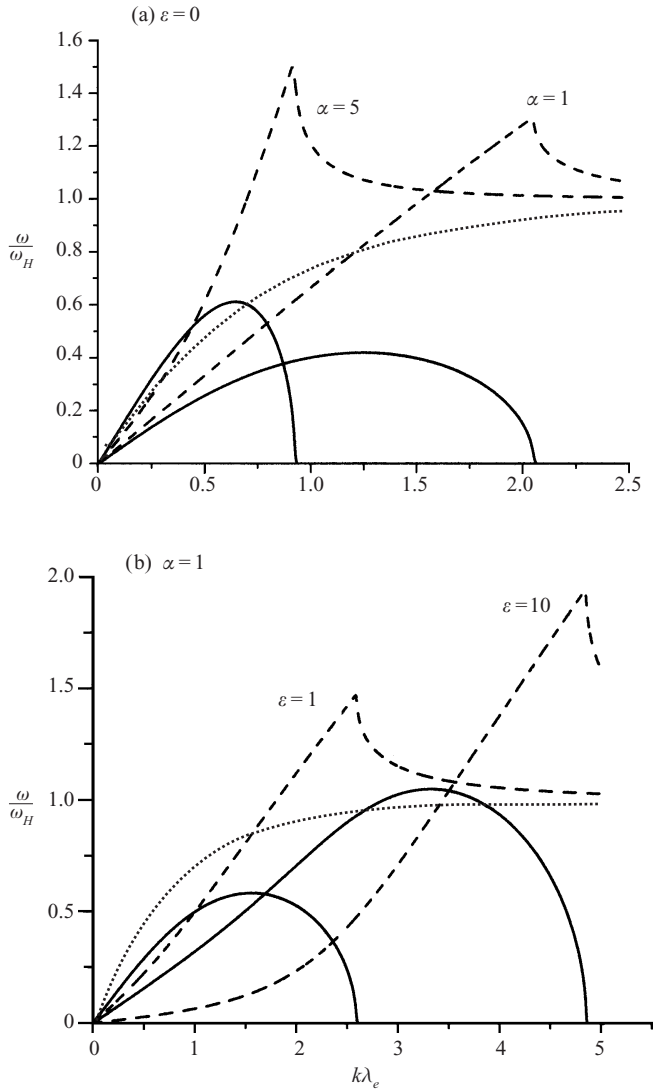

Figure 6. Growth rate (solid curves) and real frequency (dashed curves) of the wave as functions of wavelength for various α (a) and ε (b). The dotted curves show the root of the magnetosonic/lower-hybrid wave.

as $\gamma_m \approx 0.7\alpha\omega_H$, $k_m\lambda_e \approx \alpha^{-1}$, while the real frequency is nearly equal to the lower-hybrid one $\omega \approx \omega_H$. This is evidently an instability caused by the drift wave coupling with the lower-hybrid wave.

With the thermal pressure included, the dispersion equation is

$$x^3(1 + k^2\lambda_e^2) - \alpha x^2(\varepsilon - k^2\lambda_e^2) - x[1 + c_s^2(1 + k^2\lambda_e^2)] - \alpha[1 - c_s^2(\varepsilon - k^2\lambda_e^2)] = 0. \quad (4.2)$$

The first thing to point out here is that the wave stabilized by thermal pressure in the long-wavelength limit ($\varepsilon c_s^2 \geqslant 1$) becomes unstable once again at $k\lambda_e \approx \varepsilon^{1/2}$. The corresponding root $x \approx [-\alpha/(1+\varepsilon)]^{1/3}$ is quite similar to that obtained earlier. The physical reason for this can once again be understood through picturing the electron motion. At large $k\lambda_e$, the equation used in the previous qualitative analyses,

https://doi.org/10.1017/S0022377802001782 Published online by Cambridge University Press

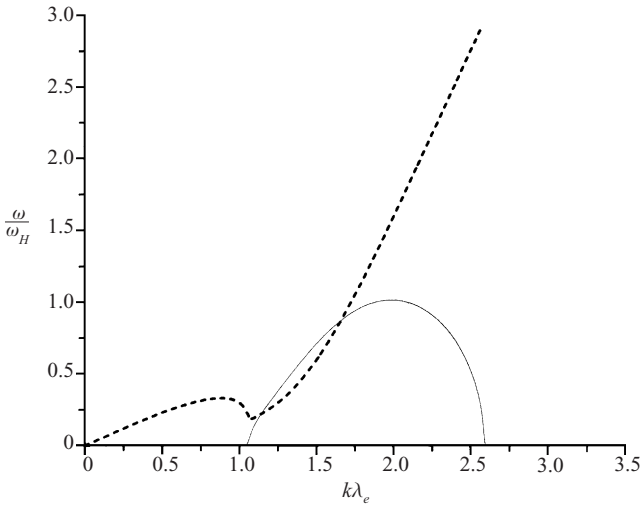

Figure 7. Plot illustrating a wave that is unstable only in the short-wavelength limit. The growth rate (solid curve) and real frequency (dashed curve) are shown. $\alpha = 3$, $\varepsilon = 3$, and $c_s^2 = 0.5$.

$\boldsymbol{\nabla} \cdot \mathbf{V}_e \approx -\partial b/\partial t$, should be replaced by

$$\boldsymbol{\nabla} \cdot \mathbf{V}_e \approx -\frac{\partial b}{\partial t} + \left(\frac{\partial}{\partial t} - V_j \frac{\partial}{\partial y} \right) \lambda_e^2 \frac{\partial^2 b}{\partial y^2}.$$

Then, taking into account all terms in the equation

$$n_0 V_{e0} \frac{\partial \rho_e}{\partial y} + V_{ex} \frac{\partial n_0}{\partial x} + n_0 \boldsymbol{\nabla} \cdot \mathbf{V}_e \approx 0,$$

one can obtain the relation

$$\rho \approx b(k^2 \lambda_e^2 - \varepsilon) - b \frac{\omega}{k V_{e0}} (1 + k^2 \lambda_e^2) \approx -b \frac{\omega}{k V_{e0}} (1 + \varepsilon).$$

This means that as $k\lambda_e \to \varepsilon^{1/2}$, the density perturbation decreases relative to magnetic field perturbation, and the thermal pressure is no longer able to stabilize the magnetic pressure. In Fig. 7, the growth rate and real frequency of this wave are shown. For a plasma near equilibrium ($\varepsilon c_s^2 \approx 1$), the maximum wavenumber scaling $k_m \lambda_e \approx \varepsilon^{1/2}$ can be expressed as $k_m r_{Le} \approx (T_i/T_e)^{1/2}$, typical of the LHDI.

The second thing to note is that the coupling with the lower-hybrid wave occurs only if the drift wave is slow, but not very slow: $C_s < V_j < V_a$. The physical reason for this is quite simple – the lower-hybrid wave cannot move slower than the thermal sound speed, so the drift wave should be at least faster than this limit. Thus, MHD instability exists only in the cold-ion limit, which can be expressed as $V_j > C_s$ rather than $\omega/k > C_s$. In the warm-ion limit (more accurately, in the warm-plasma limit, because electrons also contribute to the thermal sound speed), only kinetic instability is possible.

Short wavelengths broaden the range of inverse Landau damping as well. At sufficiently large $k\lambda_e$, kinetic instability is possible for infinitely small $\alpha \to 0$ also at $\varepsilon c_s^2 > 1$ (Fig. 4).

https://doi.org/10.1017/S0022377802001782 Published online by Cambridge University Press

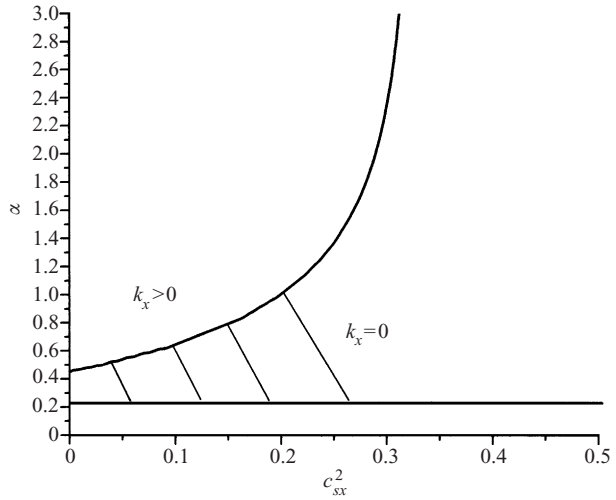

Figure 8. The ranges where cell-like ($k_x > 0$) or flute-like ($k_x = 0$) waves dominate for the case of strong temperature anisotropy ($T_y = 0$). $\varepsilon = 3$.

5. Spatial structure of the instability

Finally, we consider a topic that has not been discussed in the literature so far. It follows from (2.4) that an unstable wave may have a component k_x of the wavevector as well. Indeed, the phase velocity of the magnetosonic wave remains the same, while the drift speed viewed along the wavevector $\mathbf{k}$ slows to $V_j k_y/k$. Instability holds as long as $V_j k_y/k > V_a$. The dispersion equation in the long-wavelength and cold-plasma limits is

$$x^3 - \alpha\frac{k_y}{k}\varepsilon x^2 - x - \alpha\frac{k_y}{k} = 0, \tag{5.1}$$

where $x = \omega/kV_a$. Thus, the effect of the component k_x can be interpreted precisely as a decrease in drift speed. The increment is $\tilde{x}(\alpha k_y/k)kV_a$, where $\tilde{x}(\alpha)$ is the imaginary root of the already-discussed euqation (2.7). It follows that for a given k_y, a wave with larger k_x grows faster if $d\ \ln(\tilde{x})/d\ \ln(\alpha) < 1$. The function $\tilde{x}(\alpha)$ grows rapidly near the critical value of α and slowly at $\alpha > 1$. Far from the threshold, at any ε (either $\varepsilon \ll 1$, $\gamma = \frac{1}{2}i\sqrt{3}(\alpha k_y/k)^{1/2}kV_a$ or $\varepsilon \gg 1$, $\gamma = (-\varepsilon)^{-1/2}kV_a$), a wave with larger k_x grows faster. The range of α where unstable waves with only a component k_y dominate is quite small: $0.385 < \alpha < 0.7$. For the unstable wave that results from coupling with the lower-hybrid wave ($\alpha \ll 1$), the maximum growth rate $\gamma \approx \alpha\omega_H k_y$ is independent of k_x. This means that for a given k_y, waves with different k_x component may grow equally well.

The issue of wave structure has been mentioned by Winske (1988) while comparing results of fluid and particle numerical simulations. In general, some simulations show a cell-like structure ($k_x \approx k_y$) while others show a flute-like structure ($k_x \ll k_y$). The above analysis supports the first case. However, there is another possibility of practical importance. Let us consider the case of strong temperature anisotropy, $T_y \ll T_x$. The corresponding dispersion relation is

$$x^3 - \alpha\frac{k_y}{k}\varepsilon x^2 - \left(1 + c_{sx}^2\frac{k_x^2}{k^2}\right)x - \alpha\frac{k_y}{k}\left(1 - c_{sx}^2\frac{k_x^2}{k^2}\varepsilon\right) = 0. \tag{5.2}$$

The effect of anisotropy is most pronounced at $\varepsilon c_{sx}^2 \geqslant 1$ (Fig. 8), where the flute-

https://doi.org/10.1017/S0022377802001782 Published online by Cambridge University Press

like structure dominates over a large range of α. Note that this is not the cut-off of instability discussed earlier, because $c_{sy} = 0$.

At first glance, significant temperature anisotropy may seem unrealistic for the physical conditions for which the instability under consideration occurs. However, it may be relevant for plasma expanding into magnetic field (such as a laser-produced plasma (see e.g. Zakharov et al. 1999) or artificial releases in the Earth's magnetosphere). Typically, ions move radially with high velocity, with the thermal velocity being small in the initial stage of expansion. At later stages, when deceleration by magnetic field becomes significant, the plasma front moves slower than the ions. Thus, at the front, ions surge towards it, are reflected, and move back. The to-and-back velocity of ions at the front is roughly the local Alfvén velocity. The effective thermal sound speed $C_{sx} \approx V_a$ can be ascribed to this structure. Evidently, there is not an effective temperature T_y. Thus, the reflection of ions at the decelerating front can support a flute structure of developing instability.

It is interesting to note that the flute structure tends to be seen mainly in particle simulations. One explanation for this may be that, in this approach, counterstreaming ion flows at the front of an expanding plasma are a frequent feature, but are totally absent in the fluid approach.

6. Discussion

In view of the above analysis, the following classification seems appropriate. Instability generated by coupling of the drift wave with the magnetosonic wave extends down to the longest possible wavelengths $kL \approx 1$, while that with the lower-hybrid wave exists only in the short wavelength range $k\lambda_e \geqslant 1$, having a cut-off at the long-wavelength limit. This is a fundamental difference in view of the long-time evolution of the system, which tends to evolve from short- to long-wavelength structures. Therefore, it is proposed in this work to make a distinction between lower-hybrid drift instability (LHDI, as this instability is usually called) and magnetosonic drift instability (MSDI). There is also a kinetic type of instability that, in turn, differs from MHD instability in terms of its free-energy source and probable saturation mechanism. The main parameter that separates them, as well as the main driving force of instability, is the value of the drift speed compared with the Alfvén velocity α. The plasma temperature defines the boundary above which MHD instability may exist ($V_j > C_s$ or $\alpha > c_s$) and below which only kinetic instability is possible. Finally, the combination of parameters εc_s^2 determines the stabilizing effect of the thermal pressure on MHD instability that quenches MSDI, so that only LHDI remains. This line of reasoning is illustrated in Fig. 9. In the case of a small density gradient ($\varepsilon = 0$), there is no kinetic instability. The range of LHDI is quite small, and MSDI clearly dominates. In the case of a substantial density gradient, there appears a range of LHDI dominance at $\varepsilon c_s^2 \geqslant 1$. At $\alpha < c_s$ (warm plasma), only kinetic instability is possible. The range of MHD instability is indicated by straight line shading, while the range where there is only kinetic instability is indicated by dashed line shading. Closer spacing of shading lines indicates the ranges where instability exists only in the short-wavelength limit. It is suggested that the instability under consideration be interpreted as a current-driven instability of the plasma wave that is magnetosonic in the long-wavelength limit and lower-hybrid in the short-wavelength limit.

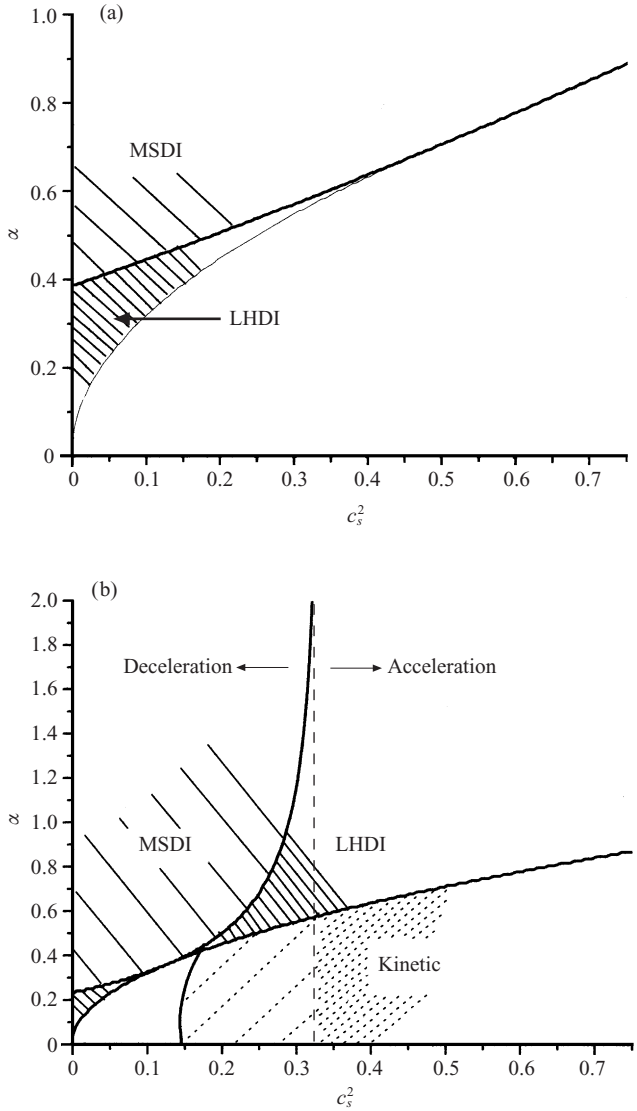

Figure 9. The ranges of lower-hybrid drift (LHDI), magnetosonic drift (MSDI), and kinetic instabilities for the cases of (a) small ($\varepsilon = 0$) and (b) substantial ($\varepsilon = 3$) density gradient. Closer spacing of the shading indicates the regions where instability exists only in the short-wavelength limit.

The line that roughly divides MSDI and LHDI ($\varepsilon c_s^2 \approx 1$) nearly coincides with the condition of the plasma being in equilibrium (with accuracy $\frac{1}{2}\gamma - 1$). This means that MSDI dominates in strongly decelerating plasmas, and LHDI in accelerating or near-equilibrium plasmas. In this sense, the proposed classification repeats that of Winske (1988): effective gravity drift or density drift LHDI. However, the notion of density drift is physically appropriate only for kinetic instability. For MHD instability, it only coincides (with accuracy $\frac{1}{2}\gamma - 1$) with the condition of strong influence of thermal pressure. Besides, in Winske (1988), the distinction between the long- and short-wavelength limits was not made. To stress

https://doi.org/10.1017/S0022377802001782 Published online by Cambridge University Press

the similarity with conventional Rayleigh–Taylor instability on the one hand and to differentiate between conventional and modified MHD equations on the other, Hassam and Huba (1987) introduced the term 'effective gravity' and ordering by the parameter ρ_i/L_n, where ρ_i is the ion Larmor radius. However, one cannot recover exact conventional MHD in either of the limits $\rho_i \to 0$ or $L_n \to \infty$. It follows from (2.4) that the parameter $\alpha = V_j/V_a = \lambda_i/L_b$ is responsible for the difference between conventional and Hall-modified MHD. Thus, the intrinsic spatial dimension of the problem is the ion plasma length $\lambda_i = c/\omega_{pi}$. The assumption that the ion Larmor radius should be larger than characteristic length is not necessary from this point of view, although it is satisfied. Indeed, in the case of strong plasma deceleration (cold ions), the Larmor radius should be calculated using the expansion velocity of the ions. To expand (with deceleration), the plasma should have a kinetic pressure greater than the magnetic pressure, which yields $\rho_i/\lambda_i > 1$. In the case of near-equilibrium or acceleration ($\varepsilon c_s^2 \geqslant 1$), it follows that $\rho_i/L_b > \varepsilon^{1/2}$.

There is one important common feature that combines all of the considered instabilities, however different they are in other respects: the maximum growth rate is always of the order of the lower-hybrid frequency. Thus, in this sense, the abbreviation LHDI is certainly most general.

7. Conclusions

In this work, we have given the modified MHD equations that describe the ion–electron drift instability of plasma a form that accentuates the basic parameters of the problem – the relation of the current speed to the Alfvén velocity and the relation of the magnetic field gradient scale to the density gradient scale. On the basis of these parameters, various features of the instability have been analyzed: physical structure, thermal pressure influence, long- and short-wavelength limits, and wavelength structure. It has been argued that the interpretation of the instability as a coupling of the drift wave with magnetosonic or lower-hybrid waves means that one should discriminate between MSDI (which has a long-wavelength limit) and LHDI (which exists only at short wavelengths), and that the cold- and warm-plasma limits that divide MHD instability from kinetic instability can be expressed in terms of plasma parameters (drift and thermal sound speeds) rather than the priori unknown wave velocity. It has been shown that long-wavelength perturbations are unstable mainly in strongly decelerating plasma, while short-wavelength perturbations are unstable in near-equilibrium or accelerating plasmas, and that the thermal pressure combined with the density gradient has a strongly stabilizing influence on long-wavelength perturbations. It has been pointed out that the instability may have a cell-like structure as well as a flute-like one, and that an effective temperature anisotropy may account for the flutes usually observed in expanding plasmas.

Acknowledgement

The author gratefully acknowledges numerous and fruitful discussions with Yu. P. Zakharov. The work was supported in part by the Russian Fund of Basic Research N02-02-17868.

References

Hassam, A. B. and Huba, J. D. 1987 *Geophys. Res. Lett.* **14**, 60.

Hassam, A. B. and Huba, J. D. 1988 *Phys. Fluids* **31**, 318–325.

Huba, J. D., Hassam, A. B. and Winske, D. 1990 *Phys. Fluids* **B2**, 1676–1697.

Krall, N. A. and Trivelpiece, A. W. 1973 *Principles of Plasma Physics*. New York: McGraw-Hill.

Winske, D. 1988 *J. Geophys. Res.* **93**, 2539–2552.

Zakharov, Yu. P., Ponomarenko, A. G., Melekhov, A. V., Posukh, V. G. and Shaikhislamov, I. F. 1999 *Trans. Fusion Technol.* **35**, 283–287.